J Mater Sci: Mater Electron (2015) 26:1419–1426
DOI 10.1007/s10854-014-2556-0

Electrical properties of silicate glasses of low level gadolinium oxide doping including dielectric and infrared measures

Reham Morsi Mohamed Morsi · Safeya Ibrahim Abd El-Ghany · Morsi Mohamed Morsi

Received: 30 September 2014 / Accepted: 25 November 2014 / Published online: 4 December 2014

Abstract Glasses of the composition (mol%) $15Na_2O$, $20CaO$, $65SiO_2$ doped with low contents of Gd_2O_3 ($0.14–0.83 \times 10^{-2}$ mol per 100 g glass) were prepared by the melt quenching method. The effect of Gd_2O_3 content on the electrical, dielectric and infrared properties of the silicate glass was studied. The Gd_2O_3 content in the silicate glass provides more non-bridging oxygen atoms into the micro structure, yet the strong field strength of Gd^{3+} ions in this glass has a counter effect that leads to a contraction in its micro structure. This contraction leads to decrease of water bands in the IR transmittance spectra. Gd_2O_3 increases the conductivity σ_{ac} which is due to ionic and electronic carriers. Variation of log σ_{ac} as a function of frequency shows a hopping frequency (ω_h) that occurs at lower frequency values as mol of Gd_2O_3 content was increased. The real part of the dielectric constant (ε') for glass containing 0.0083 mol Gd_2O_3 shows a value of 450 at 1 kHz which may make it as a promising candidate for energy storage in electronic applications.

1 Introduction

Over the last few decades, rare earth containing glasses have been attracted a great deal of interest due to their important physical and chemical properties, such as high glass transition and softening temperatures, high micro-hardness and elastic modulus, excellent chemical resistance and high thermal resistance [1–6]. Besides these specific properties, they have many applications in laboratory glassware, household cooking utensils and automobile headlamps [6]. Rare-earth doped glasses play a very significant role in the development of lasers and fiber amplifiers for optical telecommunication due to their unique properties [3, 7]. In recent years, rare-earth doped glasses have been widely studied and applied in variety of photonic applications, such as, solid-state lasers, waveguide lasers, optical fibers and optical amplifiers [8–11]. Gd_2O_3 is used in diopside-based glass system as glass ceramic sealant material for planar-solid oxide fuel cells (SOFC) [12].

Lanthanide (Ln)-doped glasses have gained much interest due to their easier synthesis compared to that of crystals [13]. Among the Ln-doped glasses, Gadolinium-containing glasses of 0.1–10 mass % are particularly interesting owing to their magnetic and optical properties [14]. Gadolinium most frequently occurs in the Gd^{3+} state with the ground state $^8S_{7/2}$; owing to the absence of orbital moment. This ion is particularly well adapted to magnetic resonance experiments. Though the local structure of the Gd^{3+} sites seems to be similar for different types of glasses, the correlation between the doping level and clustering depends on the glass type and composition [15–17].

Among the conventional glasses, soda-lime silicate glasses have attracted much attention because of their good glass forming nature compared to several other conventional systems. Silicate glass is an attractive host matrix for rare earth ions because of its fine optical and mechanical properties, such as good chemical stability, high UV transparency and low thermal expansion coefficient leading to strong thermal resistance, low non linear refractive index, high surface damage threshold, large tensile fracture strength and good durability [18, 19]. The possibility of

R. M. M. Morsi
Physical Chemistry Department, National Research Centre, Dokki, Cairo 12622, Egypt

S. I. Abd El-Ghany · M. M. Morsi (✉)
Glass Research Department, National Research Centre, Dokki, Cairo 12622, Egypt
e-mail: morsimmorsi@yahoo.com

controlling the physical properties of glasses, such as, refractive index and density by a proper variation of glass composition suggests the feasibility for chemical control of the material according to the needs for respective applications. However, there is a shortage of knowledge on the structure and properties of the multi-component soda-lime silicate glasses containing rare earth ions [20].

Mechanical properties and structure of borosilicate glasses containing rare-earth ions have been studied by many authors [21–24]. Attempts have been made to explain the change in structure of oxide glasses doped by rare earth elements and compounds, such as La_2O_3, Y_2O_3 and ErO_2 in terms of elastic constants employing ultrasonic characterizations [6, 25–27]. A significant change in structure of the glasses as a function of density has been studied through ultrasonic velocity measurements [6]. Elastic module, Debye temperature, softening temperature and Poisson's ratio have been investigated for SiO_2–Na_2O–B_2O_3 glasses doped with 0.3 up to 3.3 mol% content of Gd_2O_3 [6]. Gd_2O_3 was selected as an additive to the Na_2O–BaO–Nb_2O_5–SiO_2 (BNNS) glass–ceramic composite materials with the aim to investigate the influence of Gd_2O_3 addition on the phase transition, microstructure and dielectric properties of the BNNS glass–ceramic composites [28]. The effect of Gd and Y on the chemical durability of silicate glass has been recently investigated [29].

It is noticed that, the electrical and dielectric properties of Gd-containing glass received little attention. So, in the present study, we report the influence of very low additions of Gd_2O_3 on the electrical and dielectric properties of soda lime silicate glass of the composition (mol%) $15Na_2O$, 20CaO, $65SiO_2$. Infrared spectra of these glasses have been investigated, too.

2 Experimental

Soda lime silica glass of the composition ($15Na_2O$, 20CaO, $65SiO_2$ mol%) has been prepared by melting and quenching method. An increasing amounts of 0.14, 0. 27, 0.55 or 0.83 ($\times 10^{-2}$ mol) Gd_2O_3, per 100 g glass, were added. Table 1 lists the compositions of the glasses studied. Analytical grade sodium carbonate (Na_2CO_3), calcium carbonate ($CaCO_3$), gadolinium oxide (Gd_2O_3), and washed purified quartz silica (SiO_2) were used for the preparation of the glass batches. Melting was carried out in platinum crucibles in an electric furnace at 1350 °C and the melts were kept at this temperature for 2 h during which it was occasionally swirled out to ensure homogeneity. The melts were cast in rectangular disk forms. The samples were immediately transferred to annealing furnace at 550 °C for half an hour then it was switched off and left to cool to room temperature. Colorless glass samples were obtained.

Table 1 Nominal chemical composition of the investigated glasses

Glass no.	Glass composition (mol%)			Additives[a] (mol) $Gd_2O_3 \times 10^{-2}$
	Na_2O	CaO	SiO_2	
G_0	15	20	65	0.00
$G_{0.14}$	15	20	65	0.14
$G_{0.27}$	15	20	65	0.27
$G_{0.55}$	15	20	65	0.55
$G_{0.83}$	15	20	65	0.83

[a] Per 100 g glass

The infrared spectra of the glasses were recorded at room temperature using KBr disc technique. The spectra in the wavenumber range between 400 and 4000 cm^{-1} with a resolution of 2 cm^{-1} were obtained using a Jasco spectrometer (model FT/IR-6100).

The electrical measurements were carried out on disc shaped samples and had a thickness ranging from 1.0 to 2.0 mm. The surfaces were polished and the opposite sides for each sample were brush painted with silver paste. The painted area has a diameter of 10 mm. The sample is mounted between two stainless steel disc electrodes each 10 mm in diameter. One of the discs is kept fixed and the other disc is kept in position using perfect spring contact. Electrical connections were taken from this contact to the automatic capacitance meter. The capacitance (C) and dielectric loss factor (tan δ) of the samples were measured using LCR Hi Tester (HIOKI, 3532-50), Japan, at frequency range from 0.1 kHz to 5 MHz, and temperature range from 25 to 350 °C. The temperature was determined using a copper/Constantine thermocouple in close proximity to the sample. The temperature was measured with an accuracy of ±1 °C by means of a calibrated thermocouple connected to a digital meter. The system was working as part of computer program for processing the output from the LRC-meter and the used digital meter for measuring the temperature.

The conductivity (σ_{ac}) was obtained using the equation: $\sigma_{ac} = \omega\varepsilon''\varepsilon_o$ [30]. The dielectric constant (ε') and dielectric loss (ε'') were calculated using the following expressions [31, 32]:

$$\varepsilon' = C \cdot d / \varepsilon_o A,\ \varepsilon'' = \varepsilon' \tan\delta.$$

where C = measured capacitance of the sample (F), d = thickness of the sample (m), ε_o = permittivity of free space equals 8.85×10^{-12} F m^{-1}, A = Sample surface area (m^2), ω = the angular frequency, tan δ = the loss tangent which is obtained directly from the instrument.

3 Results and discussion

3.1 Infrared transmission spectra

The frequency of the IR-absorption peaks is sensitive to the nature and the type of the bonds [12]. The infrared spectra for the glass samples under the study are shown in Fig. 1. The bands observed in the spectra are grouped in three regions, 400–700, 700–1300 and the 1600–4000 (cm^{-1}), respectively. The first region contains the bands at 442, 477, 508 and 624 cm^{-1}. The peak at 477 cm^{-1} and the bands at 477 and 508 cm^{-1} which appear as shoulders are slightly shifted to lower wavenumbers at 455, 420 and 477 cm^{-1}, respectively, when Gd_2O_3 content is increased. In the second region the following bands and shoulders are observed:

1. A sharp band at 770 cm^{-1} which shifts to lower wavenumber at 766 cm^{-1} when the Gd_2O_3 content is increased.
2. A broad band with a peak at 1041 cm^{-1} and shoulders at 949 and 1154 (cm^{-1}). The width of this band is increased and its peak is shifted to lower wavenumber at 1032 cm^{-1} when the Gd_2O_3 content is increased.

In the third region weak bands at 1634, 2860, 2972, 3442 and 3742 cm^{-1} are recorded. The intensities of these bands are further decreased when the Gd_2O_3 content is increased.

The bands and summary of their assignments are given in Table 2. The spectrum of the Gd_2O_3-free glass G_0 (Fig. 1) shows main prominent and characteristic absorption bands originated from the silicate groups at 442, 477,

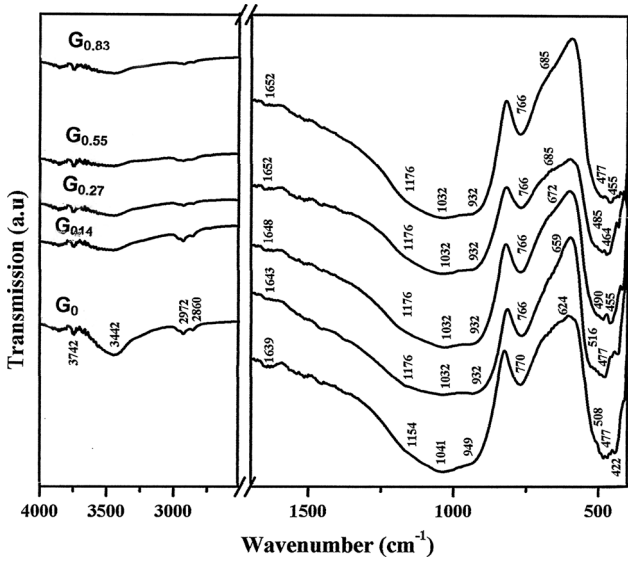

Fig. 1 Infrared spectra for glass Samples with 0.0, 0.14, 0.27, 0.55 and 0.83 ($\times 10^{-2}$ mol Gd_2O_3/100 g glass)

Table 2 IR bands and band assignment of the investigated glasses

Wavenumber (cm^{-1})	Band assignment	References
420–442	O–Si–O bending vibration mode	[36]
455–477	O–Si–O and Si–O–Si bending vibration modes	[7, 33, 37]
508–477	O–Si–O bending vibration mode	[34, 36]
624–685	Si–O–Si symmetric bending vibrations	[35, 38]
770–766	Si–O–Si symmetric stretching vibration	[7, 36, 39]
949–931	Si–O terminals asymmetric stretching vibrations	[7, 40]
1041–1032	Si–O–Si-asymmetric stretching	[7, 38, 39, 41]
1154–1176	Si–O–Si asymmetric stretching	[35]
1639–1652	Molecular water or hydroxyl-related band	[42]
2860–2927	Asymmetric and symmetric stretching modes of interstitial H_2O molecules	[42]
3442	Molecular water	[42, 44]
3742	Stretching mode of silanol Si(OH) groups	[42, 44]

508, 624,770, 949, 1041 and 1154 (cm^{-1}). The bands existing at 442, 477 and 508 cm^{-1} can be assigned to bending vibrations involving O–Si–O and Si–O–Si, characteristic of the three-dimensional network of silicate glasses [7, 33–37]. The observed band which appears as a shoulder at 624 cm^{-1} was assigned to vibrations of ring $[SiO4]^{4-}$ tetrahedral units [38] and symmetric bending Si–O–Si bonds [36, 38]. The spectrum of glass G_0 also exhibits a band located at 770 cm^{-1} which is attributed to Si–O–Si symmetric stretching vibrations of bridging oxygen between tetrahedra [7, 36, 39]. The band appeared as a shoulder located at 949 cm^{-1} in the broad band is attributed to asymmetric stretching vibration of $Si–O^-$ terminals [7, 40]. The broad band which has a peak at 1041 cm^{-1} is characteristic of asymmetric stretching vibrations of the Si–O–Si bonds [7, 36, 38–41]. The band at 1154 cm^{-1} is assigned to Si–O–Si asymmetric stretching [36] while the weak band at 1639 cm^{-1} and those at 2860, 2972, 3442 and 3742 (cm^{-1}) are assigned to the molecular water or hydroxyl group (–OH) [42–44].

The IR spectra for Gd_2O_3-doped glasses G_0–$G_{0.83}$ shown in Fig. 1 are similar to the spectrum for the undoped glass. However, it can be noticed that, doping the element (Gd^{3+}) into the glasses causes the peak at 477 cm^{-1} assigned to O–Si–O and Si–O–Si bending vibration modes to shift to lower wavenumber at 455 cm^{-1}. The bands at 1041 and 949 (cm^{-1}) are assigned to asymmetric stretching vibrations for the Si–O–Si bonds and the $Si–O^-$ terminals, respectively, also shift towards lower wavenumber. These findings are in good agreement with result reported by

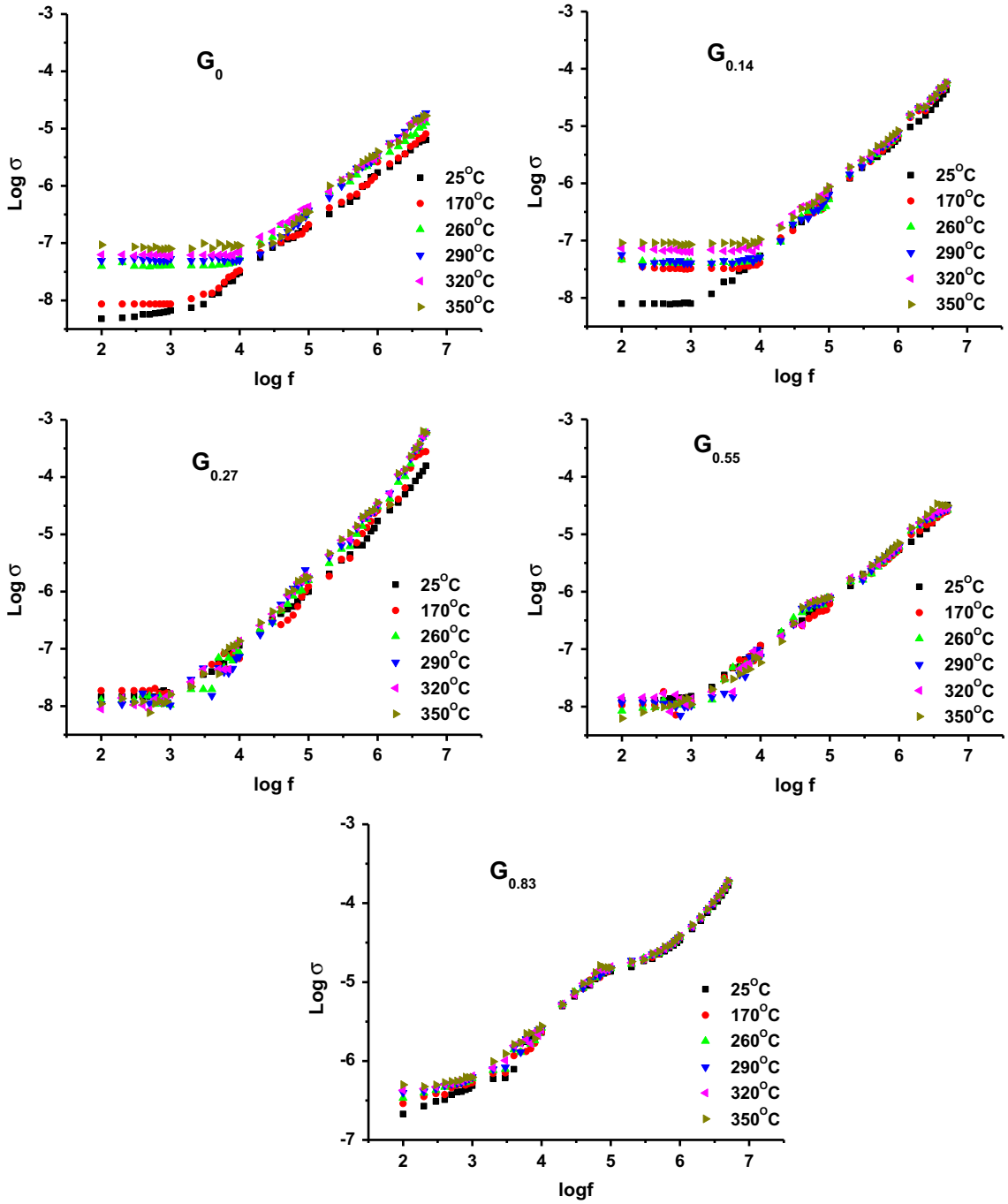

Fig. 2 Variation of σ_{ac} as a function of frequency measured at different temperatures for G_0–$G_{0.83}$ glass samples

Gaafar et al. [24], where the addition of large amount of network modifier oxides to their silicate glass leads to broadening and shifting of the corresponding bands towards lower wavenumbers. It is also reported that, rare-earth oxides including (Gd_2O_3) act as network modifier in soda-lime-silicate glass which provide non-bridging oxygens [45].

Condrate [46] reviewed the structures of glasses containing rare-earth ions on the basis of the IR vibrational spectra. The glasses discussed include silicates, phosphates, borates, halides and other structural components. The studies have interpreted the vibrational spectra assuming that rare-earth ions behave as glass network modifiers rather than as network formers. NMR and FTIR investigations [47, 48] on the rare-earth in alumino-silicate glasses have evaluated the effect of rare-earth content on the properties and structure of the glasses. The investigations reached the conclusion that the rare-earth acts as

network modifier, producing more non-bridging oxygen atoms. The broadening of the complex band in the region 900–1200 cm^{-1} is in agreement with the suggestion that adding rare-earth oxides (including Gd_2O_3) into the silicate glass causes more nonbridging oxygen to occur [45]. The observed shift of the peak positions (Fig. 1) in the range 900–1200 cm^{-1} has been attributed to the effect of variation of Gd_2O_3 content on the structure of the silicate glass [49].

The intensities of the bands due to the molecular water or hydroxyl group (–OH) (Fig. 1) are decreased while increasing the Gd_2O_3 content. This decrease in the intensities of these bands suggests the occurrence of tightening or contraction for the micro glass structure as a result of addition of Gd_2O_3. Accordingly the ability of the glass to incorporate hydroxyl group (–OH) or water molecules is decreased. Shelby [50] reported that, if the ionic radius of the modifier ions is smaller than the interstices of the network structure their attraction to the oxygen ions can lead to a decrease in the size of the interstices and consequently decreases the molar volume, i.e., causing contraction effect. Since the ionic radius of Gd^{3+} ions (0.93 Å) is smaller than that of Na^+ ions (0.98 Å) and has three positive charges, its effective field strength will exert more tightening effect causing such contraction. The strong field strength of Gd^{3+} ions in the glasses under study seems to have a counter effect that leads to a contraction in its micro structure.

3.2 Electrical and dielectric properties

Figure 2 shows the variation of log σ_{ac} as a function of frequency at different temperatures for glass samples G_0–$G_{0.83}$. A general increase in σ_{ac} is observed while increasing the frequency. It is also observed that the conductivity σ_{ac} increases with temperature particularly at low frequency regions as compared to that seen at higher frequencies.

From Fig. 2 it can also be seen that the conductivity is sharply increased above a certain frequency. This frequency is observed at 2.5, 1.3, 0.63, 0.50 or 0.11 kHz, for glasses G_0, $G_{0.14}$, $G_{0.27}$, $G_{0.55}$ or $G_{0.83}$, respectively. This frequency is conventionally known as hopping frequency (ω_h) [51, 52]. Below the hopping frequency the conductivity is frequency-independent and can be considered as plateau region (constant conductivity zone). The constant conductivity zone increases and hence, the hopping frequency (ω_h) increases too with increasing temperature (Fig. 2). For instance, it is increased from 2.5 to 10 kHz or from 1.3 to 7.9 kHz or from 0.11 to 0.45 kHz for glasses G_0, $G_{0.14}$ and $G_{0.83}$, respectively, with increasing the temperature. The present findings are consistent with the published data [53]. The increase in (ω_h) with temperature has been assigned to the release of space charges at the electrode-sample interface [52]. On the other hand, the hopping frequency (ω_h) occurs at lower frequency values as the Gd_2O_3 content is increased.

The variation of log σ_{ac} as function of frequency measured at 25 C for glasses G_0–$G_{0.83}$ is shown Fig. 3. It is observed that as Gd_2O_3 content is increased the conductivity is increased together with a shift of the hopping frequency to lower values. The later is decreased from 2.5 to 0.11 kHz for glasses G_0 and $G_{0.83}$ respectively, as Gd_2O_3 content is increased.

The variations of log σ_{ac} measured at 1 MHz as a function of reciprocal temperature for glass samples G_0–$G_{0.83}$ are shown in Fig. 4. The plots for glasses G_0–$G_{0.55}$ show the presence of two regions having different slopes, one at high temperatures and the other at relatively lower temperatures (below 77 °C). The conduction is nearly temperature-independent at the low temperature region and is temperature-dependent at the higher temperature region. Figure 4 also shows that the variation of conductivity with temperature for glass $G_{0.83}$ seems to have same rate from room temperature to higher temperature (350 °C). The conductivity σ_{ac} for glass G_0 is found to range from 1.71×10^{-6} to 3.98×10^{-6} (Ω^{-1} cm^{-1}) and increased for glass $G_{0.83}$ from 3.47×10^{-5} to 3.89×10^{-5}. The activation energy, E_{ac}, is determined from the slopes of the linear fit (Fig. 4) and listed in Table 3. From the activation energy values it can be seen that the addition of Gd_2O_3 decreases the activation energy from 0.25 eV for sample G_0 and attain the lowest value 0.03 eV for sample $G_{0.83}$, which indicates that Gd-ions play a role in the conduction mechanism. Since Na^+ ions should contribute in the electrical conduction in these glasses by the transport of Na^+

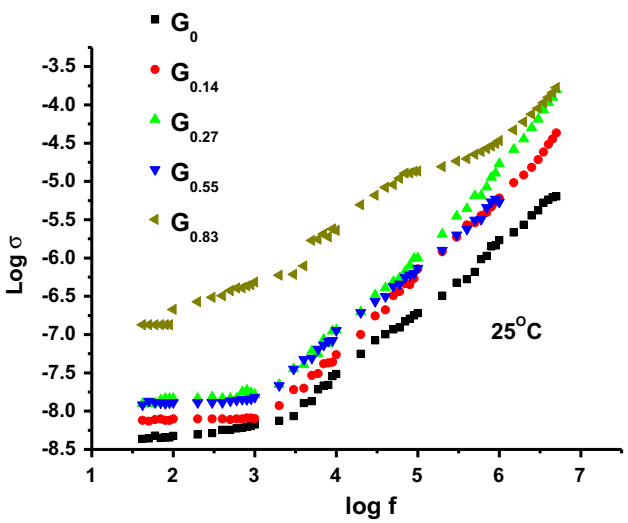

Fig. 3 Variation of σ_{ac} as function of frequency measured at room temperature for G_0–$G_{0.83}$ glass samples

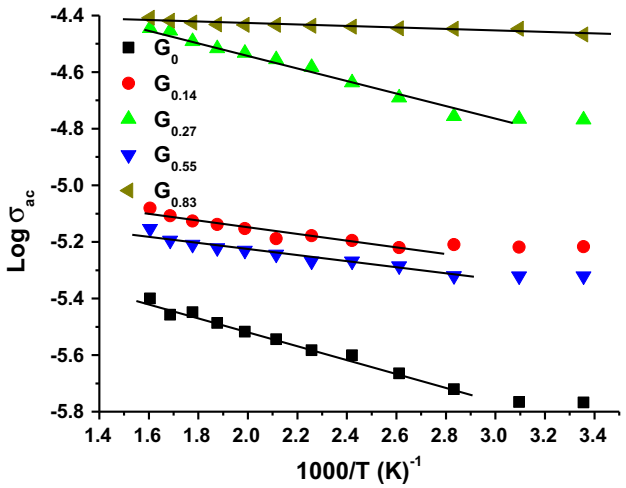

Fig. 4 Variation of σ_{ac} as a function of temperature at 1 MHz for G_0–$G_{0.83}$ glass samples

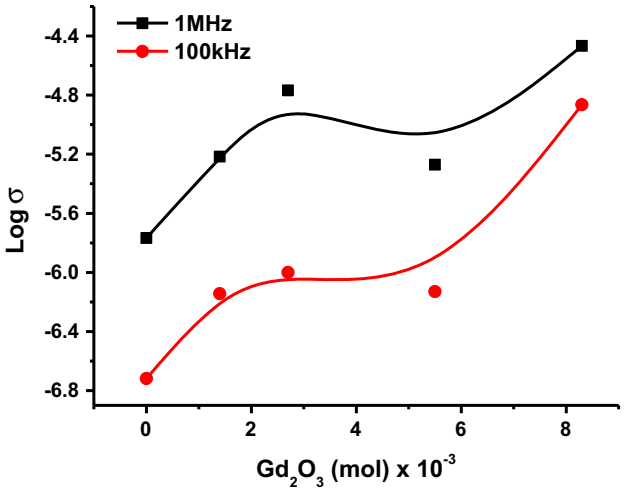

Fig. 5 Variation of conductivity σ_{ac} as function of Gd_2O_3 content measured at 1 MHz and 100 kHz at room temperature

Table 3 Dielectric constant (ε′) values measured at 1 kHz and 1 MHz and Ac activation energy (E_{ac}) of samples studied

Glass no.	ε′ (at 1 kHz)		ε′ (at 1 MHz)		E_{ac} (eV)
	25 °C	350 °C	25 °C	350 °C	
G_0	11	48	3	3	0.25
$G_{0.14}$	17	50	11	15	0.11
$G_{0.27}$	20	51	11	19	0.22
$G_{0.55}$	24	30	7	12	0.11
$G_{0.83}$	450	567	57	64	0.03

ions through the glassy network, thus, the conduction in the studied glasses seems to occur by electronic and ionic carriers.

Figure 5 shows the variation of conductivity σ_{ac} as function of Gd_2O_3 content measured at 1 MHz and 100 kHz at room temperature. The increase in conductivity σ_{ac} as Gd_2O_3-content is increased indicates that Gd-ions may cause structural deformations that affect the electrical properties. The effect of Gd-ions seems to have two folds, increasing the non bridging oxygens and contracting the micro structure of the glass. The first effect is elucidated by the observed increase in conductivity. The second effect is expected to cause obstruction for the mobility of the Na^+ ions that results in decreasing the conductivity. With further increase of Gd_2O_3 content the contribution of Gd-ions in the conductivity mechanism is increased, consequently the increase in conductivity is restored, which explains the observed non linear behavior recorded in Fig. 5.

The dielectric constant (ε′) values plotted as a function of temperatures for glasses G_0–$G_{0.83}$ measured at various frequencies are shown in Fig. 6. This figure shows an increase in the dielectric constant values while increasing temperature, especially for measurements performed at low frequencies (1 and 10 kHz). The increase in ε′ with increasing temperature is predicted to occur due to the weakening in binding force between molecules/atoms, permitting the molecules/atoms to vibrate more and more which in turn increases the polarization, hence increasing the dielectric constant (ε′) [52, 54]. Addition of Gd_2O_3 content seems to cause structural changes that facilitate vibration of molecules/atoms as a result of introducing non bridging oxygen atoms to the system (as proved from IR data). Consequently an increase in the polarization increases the dielectric constant (ε′).

The results obtained for the dielectric constants (Fig. 6) are summarized in Table 3, where the (ε′) values measured at low (≤1 kHz) and high (≤1 MHz) frequencies at 25 and 350 °C are compared. It is observed that the values of dielectric constant measured at 1 kHz are higher than those for the corresponding values measured at 1 MHz. For example, the dielectric constants (ε′) for glass G_0 measured at 25 °C and at 1 kHz or 1 MHz attained values of 11 and 3, respectively, whereas for glass $G_{0.83}$ the values obtained are 450 and 57, respectively. This observation is probably related to space charge/interfacial polarization at lower frequencies [52, 54].

4 Conclusions

1. Doping soda-lime-silicate glass with Gd_2O_3 provides more non-bridging oxygen atoms, yet the strong field strength of Gd^{3+} ions seems to cause a counter effect that leads to a contraction in the glass structure. The decrease of water bands in the IR spectra of glass containing Gd_2O_3 confirms the occurrence of structure contraction that decreases the ability of the glasses for water absorption.

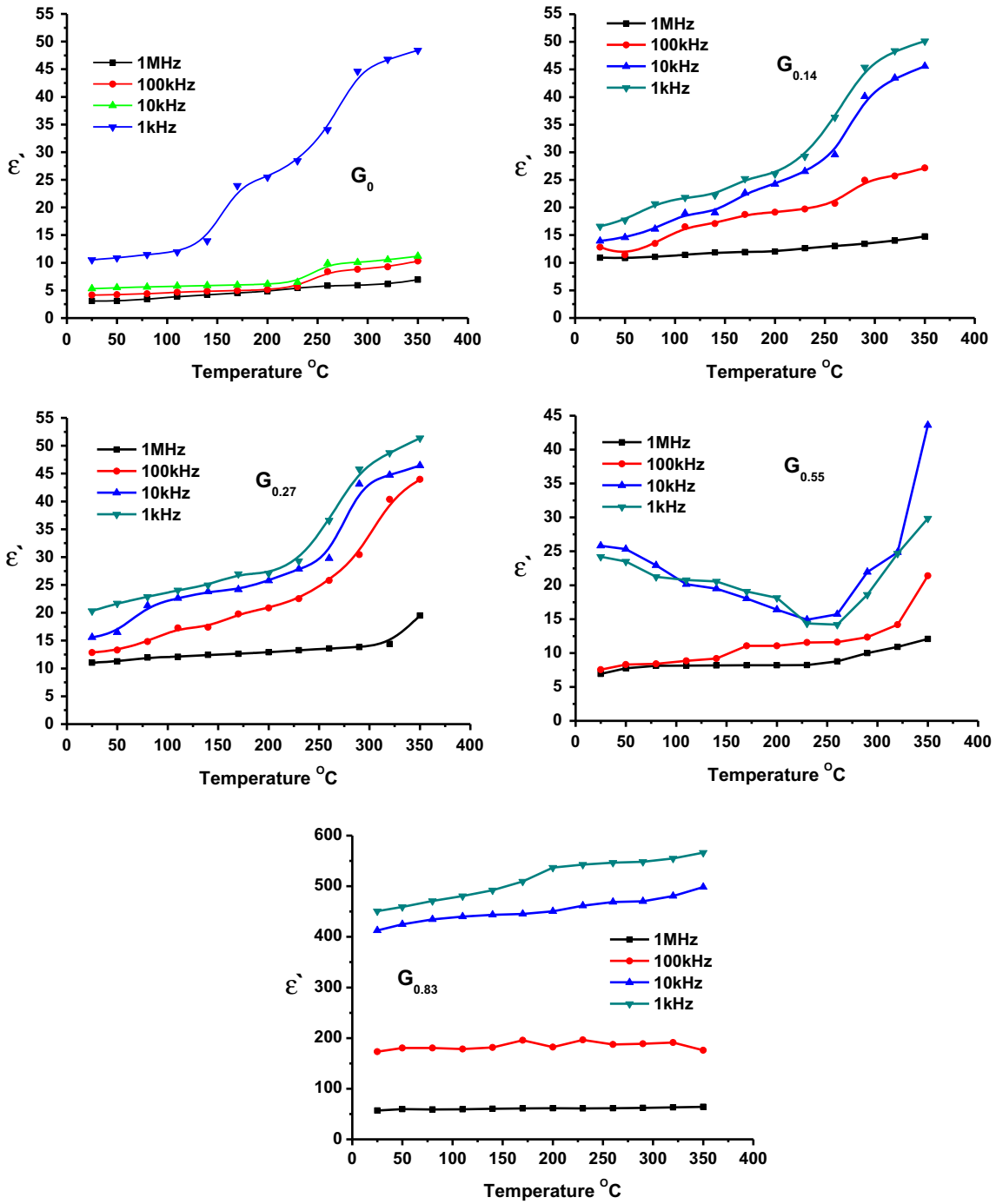

Fig. 6 Dielectric constant as a function of temperatures for G_0–$G_{0.83}$ glasses measured at different frequencies

2. Doping of glass with low level Gd_2O_3 increases the σ_{ac} conductivity which occurs by ionic and electronic carriers.
3. Addition of Gd_2O_3 increases the dielectric constant (ε') to reaches a value of 450 at 25 °C and 1 kHz for glass with 0.0083 mol Gd_2O_3. This result indicates that Gd_2O_3-doped glass may make it as a promising candidate for energy storage in electronic applications. The present application could be added as a new application to the commonly known applications of Gd_2O_3 containing glasses in optical applications.

References

1. M.T. Wang, J. Cheng, M. Li, F. He, W. Deng, Solid State Sci. **14**, 1233 (2012)
2. M. El-Okr, M. Ibrahem, M. Farouk, J. Phys. Chem. Solids **69**, 2564 (2008)

3. J. Johnson, R. Weber, M. Grimsditch, J. Non Cryst. **35**, 1650 (2005)
4. F. Lofaj, R. Satet, M.J. Hoffmanna, A.R. de Arellano Lopez, J. Eur. Ceram. Soc. **24**, 3377 (2004)
5. S. Hampshire, M.J. Pomeroy, J. Non Cryst. Solids **344**, 1 (2004)
6. S.Y. Marzouk, Phys. B **405**, 3395 (2010)
7. M.T. Wang, J.S. Cheng, M. Li, F. He, Phys. B **406**, 187 (2011)
8. W. Kaewwiset, K. Thamaphat, J. Kaewkhao, P. Limsuwan, Phys. B **409**, 24 (2013)
9. H. Lin, K. Liu, E.Y.B. Pun, T.C. Ma, X. Peng, Q.D. An, J.Y. Yu, S.B. Jiang, Chem. Phys. Lett. **398**, 146 (2004)
10. Y.K. Sharma, S.S.L. Surana, R.K. Singh, R.P. Dubedi, Opt. Mater. **29**, 598 (2007)
11. H.X. Yang, H. Lin, L. Lin, Y.Y. Zhang, B. Zhai, E.Y.B. Pun, J. Alloy Compd. **453**, 49 (2008)
12. A.A. Reddy, N. Eghtesadi, D.U. Tulyaganov, M.J. Pascual, L.F. Santos, S. Rajesh, F.M.B. Marques, J.M.F. Ferreira, Eur. Ceram. Soc. **34**, 1449 (2014)
13. K. Srinivasulu, I. Omkaram, H. Obeid, A. Suresh Kumar, J.L. Rao, J. Mol. Struct. **1036**, 63 (2012)
14. J. Kliava, I. Edelman, A. Potseluyko, E. Petrakovskaja, R. Berger, I. Bruckental, Y. Yeshurun, A. Malakhovskii, T. Zarubina, J. Magn. Mater. **272–276**, 1647 (2004)
15. I.V. Chepeleva, V.N. Lazukin, S.A. Demdovskii, Sov. Phys. Dokl. **11**, 86 (1967)
16. C.M. Brodbeck, L.E. Iton, J. Chem. Phys. **83**, 4285 (1985)
17. L. Cugunov, A. Mednis, J. Kliava, J. Phys. Condens. Matter **3**, 8017 (1991)
18. Y. Qiao, N. Da, P. Mingying, Y. Lyun, C. Danping, Q. Jianrong, Z. Congshan, T. Akai, J. Rare Earths **24**, 765 (2006)
19. Q. Zhou, L. Xu, L. Liu, W. Wang, C. Zhu, F. Gan, Opt. Mater. **25**, 313 (2004)
20. P. Chimalawong, J. Kaewkhao, C. Kedkaew, P. Limsuwan, J. Phys. Chem. Solids **71**, 965 (2010)
21. A. Abd El-Moneim, Phys. B **325**, 319 (2003)
22. K. El-Egili, Phys. B **325**, 340 (2003)
23. L.G. Protasova, V.G. Kosenko, Glass Ceram. **60**, 164 (2003)
24. M.S. Gaafar, S.Y. Marzouk, Phys. B **388**, 294 (2007)
25. J. Johnson, R. Weber, M. Grimsditch, J. Non Cryst. Solids **35**, 650 (2005)
26. L.G. Hwa, T.H. Lee, S.P. Szu, Mater. Res. Bull. **39**, 33 (2004)
27. Y. Vaills, Y. Luspin, G. Hauret, B. Cote, Solid State Commun. **87**, 1097 (1993)
28. Yi Zhou, Q. Zhang, J. Luo, Q. Tang, J. Du, Scr. Mater. **65**, 296 (2011)
29. L. Mei, J. Cheng, F. He, Z. Liu, Y. Hu, J. Nucl. Mater. **433**, 287 (2013)
30. M.M. EL-Desoky, J. Mater. Sci. Mater. Electron. **9**, 447 (1998)
31. P.B. Macedo, C.T. Moynihan, R. Bose, Phys. Chem. Glasses **13**, 171 (1972)
32. J.C. Anderson, *Dielectrics* (Chapman and Hall Ltd., London, 1964), p. 171
33. C. Bootjomchai, J. Laopaiboon, S. Nontachat, U. Tipparach, R. Laopaiboon, Nucl. Eng. Des. **248**, 28 (2012)
34. A.M.B. Silva, C.M. Queiroz, S. Agathopoulos, R.N. Correia, M.H.V. Fernandes, J.M. Oliveira, J. Mol. Struct. **986**, 16 (2011)
35. M. M. Mahmoud, Ph.D. Thesis, Faculty of the Virginia Polytechnic Institute and State University, Blacksburg, Virginia, (2007)
36. N.A. Al-Alaily, Glass Technol. **44**, 30 (2003)
37. M.M. Morsi, A.W. El-Shennawi, Phys. Chem. Glasses **25**, 64 (1984)
38. T.G.V.M. Rao, A.R. Kumar, M.R. Reddy, J. Non Cryst. Solids **358**, 25 (2012)
39. Y. Li, K. Liang, J. Cao, B. Xu, J. Non Cryst. Solids **356**, 502 (2010)
40. K. Annapurna, M. Dasa, P. Kundua, R.N. Dwivedia, S. Buddhudu, J. Mol. Struct. **741**, 53 (2005)
41. S. Feller, G. Lodden, A. Riley, T. Edwards, J. Croskrey, A. Schue, D. Liss, D. Stentz, S. Blair, M. Kelley, G. Smith, S. Singleton, M. Affatigato, D. Holland, M.E. Smith, E.I. Kamitsos, C.P.E. Varsamis, E. Ioannou, J. Non Cryst. Solids **356**, 304 (2010)
42. K. Singh, I. Bala, V. Kumar, Ceram. Int. **35**, 3401 (2009)
43. G. Navara, J. Non Cryst. Solids **351**, 1796 (2005)
44. G. Navara, J. Non Cryst Solids **353**, 555 (2007)
45. M.T. Wang, J. Cheng, J. Alloys Compd. **504**, 273 (2010)
46. R.A. Condrate, Key Eng. Mater. **94–95**, 209 (1994)
47. N.J. Clayden, S. Esposito, A. Aronne, P. Oernice, J. Non Cryst. Solids **258**, 11 (1999)
48. S.L. Lin, C.S. Hwang, J. Non Cryst. Solids **202**, 61 (1996)
49. M. Wang, M. Li, J. Cheng, F. He, J. Mol. Struct. **1063**, 139 (2014)
50. J.E. Shelby, *Introduction to Glass Science and Technology*, 2nd edn. (The Royal Society of Chemistry, Cambridge, U.K, 2005), p. p77
51. S. Brahma, R.N.P. Choudhary, A.K. Thakur, Phys. B **355**, 188 (2005)
52. M. Goswami, S.K. Deshpande, R. Kumar, G.P. Kothiyal, J. Phys. Chem. Solids **71**, 739 (2010)
53. S. Dahiya, R. Punia, S. Murugavel, A.S. Maan, Indian J. Phys. **8811**, 1169 (2014)
54. R.M.M. Morsi, M.A.F. Basha, Mater. Chem. Phys. **129**, 1233 (2011)